Reversible Reactions of Thiols and Thiyl Radicals with Nitrone Spin Traps

Dmitrii I. Potapenko,[†] Elena G. Bagryanskaya,[†] Yuri P. Tsentalovich,[†] Vladimir A. Reznikov,[‡] Thomas L. Clanton,[||] and Valery V. Khramtsov*[,§,||]

International Tomography Center, Novosibirsk 630090, Russia, Institute of Organic Chemistry, Novosibirsk 630090, Russia, and Institute of Chemical Kinetics & Combustion, Novosibirsk 630090, Russia, and Dorothy M. Davis Heart & Lung Research Institute, The Ohio State University, 201 HLRI, 473 W 12th Ave, Columbus, Ohio 43210

Received: March 3, 2004

The reactions of the reversible addition of thiols and thiyl radicals to the nitrone spin traps DMPO (5,5-dimethyl-1-pyrroline *N*-oxide) and DEPMPO (5-diethoxyphosphoryl-5-methyl-1-pyrroline *N*-oxide) are described. Addition of the thiols to the double C═N bond of the nitrones results in the formation of the corresponding hydroxylamines, measured using ^{31}P NMR and the phosphorus-containing trap DEPMPO. Subsequent mild oxidation of these hydroxylamines into the paramagnetic adducts may interfere with genuine spin trapping of thiyl radicals representing the Forrester−Hepburn mechanism. The reverse decomposition of hydroxylamines to the parent nitrone and thiol and of paramagnetic adducts to the nitrone and thiyl radical were observed for the first time. The recycling of reduced thiols from thiyl radicals by nitrones may comprise the mechanism of their effective antioxidant activity, in vivo. The release of thiyl radicals upon the breakdown of the paramagnetic adduct may significantly affect not only the quantitative analysis of the spin trapping data but even the conclusions regarding the origin of short-lived radical intermediates. The equilibrium constant for the reactions of the formation of the product of DEPMPO with S-centered nucleophiles decreases in the series: sulfite > thioglycolic acid > cysteine > glutathione. The rate constants for the reaction of the monomolecular decomposition of the radical adducts back to the nitrone and glutathiyl radical were found to be equal to 0.3 ± 0.1 s^{-1} and 0.02 s^{-1} for DMPO/GS$^{\bullet}$ and DEPMPO/GS$^{\bullet}$ radical adducts, correspondingly.

Introduction

The chemistry of nitrones has significant interest due to their wide applications as spin traps for EPR detection of short-lived radical intermediates in biological systems[1,2] and their growing applications as therapeutic agents.[3,4] Recently we observed new reversible nonradical reactions of the nitrone spin traps 5,5-dimethyl-1-pyrroline *N*-oxide (DMPO)[5] and 5-diethoxyphosphoryl-5-methyl-1-pyrroline *N*-oxide (DEPMPO)[6] with (bi)-sulfite forming the corresponding hydroxylamine compounds. Mild oxidations of these compounds lead to the formation of the radical adducts, identical with those obtained by genuine EPR spin trapping. This reaction might also be of importance with respect to the therapeutic activity of nitrones, taking into account sulfite toxicity,[7,8] particularly for patients with sulfite hypersensitivity.[9]

The ability of nitrones to undergo nucleophilic addition by (bi)sulfite anions opens a critical question whether similar reactions may proceed with other S-centered anions of biological importance, e.g. anions of glutathione (GSH) or cysteine (CySH). To answer this question, we have used the NMR-spin trapping approach, which is ideally suited for studies of EPR-invisible diamagnetic products formed in the reactions of nitrones with nucleophiles[5,6]. In a complimentary way, EPR spin trapping has been used to evaluate alternative pathways of the diamagnetic product formation due to the decay of EPR-detectable paramagnetic adducts of nitrones with thiyl radicals. Our data support the existence of reversible nucleophilic addition of thiols to nitrone spin traps. Surprisingly, we also observed the reversibility of thyil radical adition to the nitrones and, for the first time, demonstrate monomolecular decomposition of the corresponding adducts back to thyil radicals and the parent nitrone. The findings provide a more complete understanding of the possible biological activity of nitrones and provide evidence for largerly overlooked reactions that necessitate a reinterpretation of the many EPR spin trapping experiments.

Materials and Methods

Chemicals. DMPO, DEPMPO, diethylenetriaminepentaacetic acid (DTPA), disodium and monopotassium phosphate, Chelex-100, cysteine, GSH, oxidized glutathione (GSSG), sodium nitrite, formic and thioglycolic acid were obtained from Sigma. DMPO was distilled under vacuum. nitrosocysteine (CySNO) was synthesized according to ref 10. Nitrosothioglycolic acid (AcSNO) was synthesized by combining an equimolar concentration of thioglycolic acid (AcSH) with sodium nitrite in 0.2 N HCl. After that up to 0.1 M of the sodium phosphate was added, and the solution was titrated to pH 7.0. Nitrosoglutathione was synthesized as described in the literature[11] and stored in a freezer. Sodium formate was obtained by neutralization of formic acid by NaOH and dried afterward. For all measurements, deionized water was used. Phosphate buffer was passed through column with Chelex-100 to remove trace amounts of transition metal ions.

* Corresponding author. Tel. (614) 688-3664. Fax (614) 293-4799. E-mail: khramtsov-1@medctr.osu.edu.
[†] International Tomography Center.
[‡] Institute of Organic Chemistry.
[§] Institute of Chemical Kinetics & Combustion.
[||] The Ohio State University.

10.1021/jp049026t CCC: $27.50
Published on Web 05/29/2004

NMR Measurements. NMR spectra were measured with a Bruker AVANCE 200 spectrometer in 5 mm tubes. In ^{31}P NMR experiments, D_2O and thioglycolic acid were added to 0.2 M phosphate buffer, 0.5 mM DTPA. The mixture was titrated to pH 7.0, DEPMPO was added afterward, and ^{31}P NMR spectra were measured. The final concentration of D_2O in the sample was about 10% to perform a lock standard $\pi/2$ pulse sequence with ^{1}H decoupling. The number of scans was from 100 to 512, the sweep width was 50 ppm, LB = 0.5, the acquisition time was 8.074 s, and the delay between scans was 15 s.

^{1}H NMR spectra were registered in D_2O solution. Na_2HPO_4, DTPA, and thioglycolic acid were dissolved in deuterium oxide, and the solution was titrtrated to pH_{obs} 6.58, which corresponds to pD = 7.0.[12] DEPMPO was added afterward, and ^{1}H NMR spectra were measured. A standard $\pi/2$ pulse sequence was used. Typical settings were as following: sweep width, 10 ppm; acquisition time, 8.179 s; number of scans, 32; delay between scans, 5 s.

EPR Measurements. EPR measurements were carried out using a Bruker EMX spectrometer with a quartz flat cell, 0.25 mm thickness, or 1 mm quartz capillaries. The spectrometer settings were as following: modulation amplitude, 1.0 G; sweep width, 80 G for DMPO or 120 G for DEPMPO experiments, correspondingly; frequency, 10.05 GHz; modulation frequency, 100 kHz; microwave power, 5.19 mW; time constant, 81.92 ms; sweep time, 41.94 s. An eximer Xe−Cl laser with pulse power of about 30 mJ per pulse, 308 nm wavelength, was used as the light source in kinetic studies. Radical adduct concentration was determined relative to the integral signal intensity of the stable nitroxyl radical, 3-carboxy-2,2,5,5-tetramethylpyrrolidine-1-yloxy, measured at the same settings. To study the possible influence of the dissolved oxygen on the kinetics, the measurements of the air-saturated and argon-bubbled (30 min) samples were performed.

UV Lamp Photolysis. Photolysis was performed using a high-pressure mercury lamp, 500 W, in a quartz cell with optical path 1.0 cm. The wavelengths band from 500 to 600 nm was selected using light filters. The samples containing 10 mM nitrosothiol, 42.5 mM DEPMPO in 0.1 M phosphate buffer, pH 7.0, 10% D_2O, were irradiated with light intensity 15 mW/cm^2 during 1.5 h. The solution was bubbled by Ar for the period of time starting 10 min before the irradiation and until the end of photolysis. The spectrophotometric measurements showed about 90% of light-induced decomposition of the nitrosothiols. ^{31}P NMR spectra were measured after irradiation and compared with those measured before irradiation.

Laser Photolysis. A Nd:YAG laser (wavelength 532 nm, power 30 mJ per pulse, frequency 25 Hz, irradiated sample area, 1 cm^2) was used as a light source. The 2 mL solution of the GSNO and DEPMPO in 0.1 M phosphate buffer was irradiated during 30 min in a quartz cell with optical path 1 cm. The solution was bubbled by Ar for the period of time starting 10 min before the irradiation and until the end of photolysis. After irradiation the solution was transferred to a NMR tube and the ^{31}P NMR spectrum was measured.

Laser Flash Photolysis (LFP). A detailed description of the LFP equipment has been published previously[13,14]. Solutions in a rectangular cell (10 mm × 10 mm) were irradiated with a Lambda Physik EMG 101 excimer Xe−Cl laser (308 nm, pulse energy up to 100 mJ, pulse duration 15−20 ns). The dimensions of the laser beam at the front of the cell were 3 mm × 8 mm. The monitoring system includes a DKSh-150 xenon short-arc lamp connected to a high current pulser, a homemade monochromator, a 9794B photomultiplier (Electron Tubes Ltd.), and a LeCroy 9310A digitizer. The monitoring light, focused in a rectangle of 3 mm height and 1 mm width passed through the cell along the front (laser irradiated) window. Thus, in all experiments the excitation optical length was 1 mm, and the monitoring optical length was 8 mm. All solutions were bubbled with argon starting 15 min prior to and during irradiation. The experiments were carried out at room temperature in 0.1 M phospate buffer, pH 7.0.

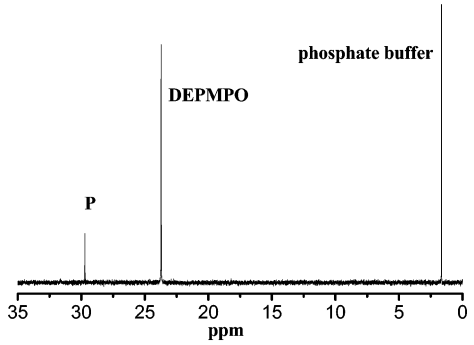

Figure 1. ^{31}P NMR spectrum of the reaction mixture of DEPMPO and thioglycolic acid in 0.1 M phosphate buffer. First, 0.2 M Na_2HPO_4, 0.5 mM DTPA, and 576 mM AcSH were dissolved in D_2O solution and the mixture was titrated to pH_{obs} = 6.58. Afterward, 42.5 mM DEPMPO was added and ^{31}P NMR spectrum was measured. Number of scans, four.

TABLE 1: Values of pK = −log K_{NuH} for the Series of S-centered Nucleophiles and Estimates of the Product K_p = $K_{NuH}K_{ad}K_b$ for Their Corresponding Reactions of Nucleophilic Addition to Nitrone Spin Traps DMPO and DEPMPO, Generalized in Eqs 23−25

spin trap	NuH	pK_{NuH}	K_p, M^{-1}	ref
DMPO	HSO_3^-	7.2	18	5
DEPMPO	HSO_3^-	7.2	132,[a] 257[b]	6
DEPMPO	$HSCH_2COO^-$	10.05	0.14	this work
DEPMPO	CysSH	8.35	≈0.03	this work
DEPMPO	GSH	9.0	<0.003	this work

[a] Trans-addition. [b] Cis-addition.

Results

^{31}P NMR Studies of Nucleophilic Addition of Thiols to the Spin Trap DEPMPO. Figure 1 shows ^{31}P NMR spectrum of the reaction mixture of 288 μmol of thioglycolic acid and 21.3 μmol of DEPMPO in 0.5 mL of phosphate buffer in D_2O, pH_{obs} = 6.58. The appearance of the new line at 29.72 ppm indicates the formation of a new diamagnetic product, P, in the amount of 1.65 μmol with a corresponding decrease of the DEPMPO signal down to 19.6 μmol.

The identical spectra were obtained in air-saturated and Ar-bubbled buffer solutions, in the absence of the oxidants, therefore favoring a nonradical mechanism for the reaction. The dilution of the sample three times resulted in a proportional decrease of the product P down to 0.55 μmol. The results are also consistent with recycling of the DEPMPO, increasing to 20.7 μmol, from backward transformation of the product P to the parent DEPMPO. Figure 2 shows that the concentration of the product P is directly proportional to the concentrations of DEPMPO and thioglycolic acid, supporting an equilibrium between parent DEPMPO, AcSH, and DEPMPO/AcSH adduct (see Figure 2 captions and Table 1 for the equilibrium constant).

The above observation is qualitatively identical to the previously described reversible reaction of DEPMPO with (bi)-sulfite, resulting in the formation of a hydroxylamine deriva-

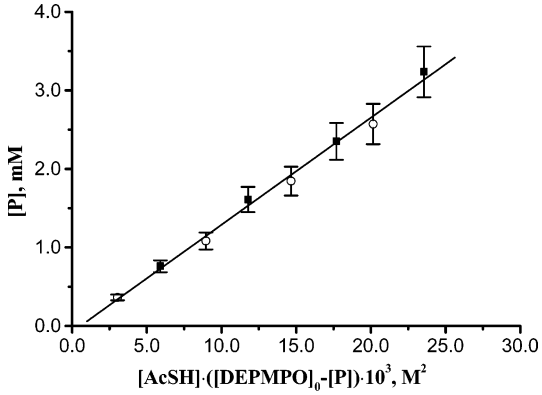

Figure 2. Dependence of the concentration of diamagnetic product P on the DEPMPO and thioglycolic acid concentrations. AcSH was added to 0.2 M phosphate buffer solution, 0.5 mM DTPA, 10% D_2O. The mixture was titrated to pH 7.0 and then DEPMPO was added and the ^{31}P NMR spectrum was measured. Number of scans was from 100 to 512, depending on the concentration of the product P. (○) Variation of AcSH concentration at initial DEPMPO concentration, $[DEPMPO]_0 = 42.5$ mM; (■) variation of DEPMPO concentration at initial AcSH concentration, $[AcSH]_0 = 288$ mM. The excellent linear extrapolation of the data is in agreement with eq 26, namely, $[P]/[DEPMPO] = K_{NuH}K_{ad}K_b[AcSH]$, yielding $K_{NuH}K_{ad}K_b = 0.14 \pm 0.1\ M^{-1}$ (see Discussion).

tives.[6] Therefore, in a similar way, we assigned the product P to the corresponding hydroxylamine of DEPMPO, namely [5-(diethoxyphosphoryl)-5-methyl-1-oxy-4,5-dihydro-3*H*-pyrrol-2-ylthio]acetic acid, formed by addition of the sulfur group of thioglycolic acid to the double bond of the nitrone by reaction 1 (RSH = AcSH):

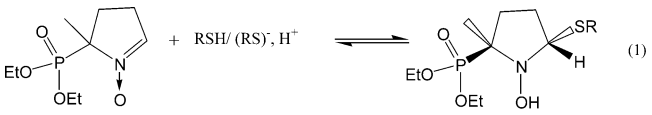

(1)

DEPMPO P (RSH = HSO_3^- [6], AcSH, GSH, CySH)

The value of the ^{31}P NMR chemical shift of the compound P is approximately 30 ppm, which is typical for DEPMPO hydroxilamine derivatives.[6,15]

In similar experiments using DEPMPO and cysteine, an appearance of several additional ^{31}P NMR signals were observed in the region 29−32 ppm, characteristic for DEPMPO hydroxylamine derivatives,[6,15] with total integral intensity being directly proportional to the concentrations of DEPMPO and CySH (data not shown, see Table 1 for the estimate of equilibrium constants). However, their quantitative analysis was not possible, due to low product concentrations. NMR spectra of the DEPMPO mixture with GSH did not reveal any additional diamagnetic products. One possible explanation of this fact could be the lower equilibrium constant for the reaction of DEPMPO with GSH and, therefore, a lower equilibrium concentration of the adduct, DEPMPO/GSH, being below the ^{31}P NMR threshold of detection.

EPR and ^{31}P NMR Detection of the Adducts from Reactions of Nitrone Spin Traps with Thiyl Radicals. Reversibility of the reaction of nitrones with thiols provides a unique detoxification mechanism of thiyl radicals by these spin traps. This possibility is made more likely by the fact that the main pathway of the decay of the paramagnetic adducts of the nitrones with RS• in biological systems is their reduction to the corresponding hydroxylamines. Therefore, following decomposition of the hydroxylamine back to nitrone and RSH will result in thiol recycling.

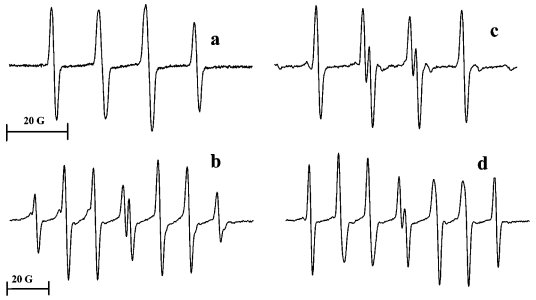

Figure 3. EPR spectra obtained under laser photolysis at 308 nm of 5 mM GSNO (a, b) or 5 mM AcSNO (c, d) in the presence of 88.5 mM spin trap (a, c, DMPO; b, d, DEPMPO) in 0.1 M phosphate buffer, pH 7.0. Laser frequency was 4 Hz, and the number of scans four. The hyperfine splittings determined by EPR spectra simulations are $a_N = 15.12$ G, $a_H = 16.11$ G (a); $a_P = 45.81$ G, $a_N = 14.14$ G, $a_H = 14.94$ G (b); $a_N = 15.19$ G, $a_H = 16.92$ G (c); $a_P = 46.57$ G, $a_N = 14.26$ G, $a_H = 15.53$ G (d).

To test this hypothesis, we used the photolysis of the nitrosothiols GSNO and AcSNO, both by UV lamp and laser in the presence of spin traps DEPMPO or DMPO. The photolysis of nitrosothiols leads to the formation of thiyl radicals via homolitic cleavage of the S−N bond:[16−19]

$$RSNO \xrightarrow{h\nu} RS^\bullet + NO^\bullet \qquad (2)$$

In the presence of nitrone spin trap, ST, thiyl radical, RS•, is effectively scavenged with the formation of the radical adduct, ST/RS•:

$$RS^\bullet + ST \xrightarrow{k_{st}} ST/RS^\bullet \qquad (3)$$

Figure 3 demonstrates the EPR spectra of the adducts of DMPO (a, c) and DEPMPO (b, d) with GS• and AcS• radicals generated via photolysis of the GSNO and AcSNO, correspondingly. The spectral parameters of the adducts with GS• radical (see Figure 3 caption) coincide with the literature data for DMPO/GS• and DEPMPO/GS• adducts,[16,20] while these parameters for the adduct with AcS• are described here for the first time. The reduction of the adduct, ST/RS•, will result in the formation of the corresponding hydroxylamine, HA−SR. The same compound, HA−SR, as well as the nitrone, N−SR, are formed due to a second-order disproportionation reaction:[15]

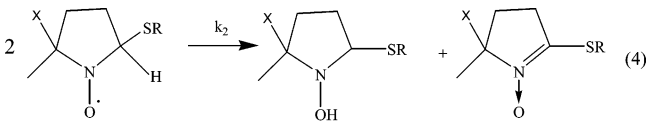

(4)

ST/RS• HA-SR

If the reversibility of the reaction 1 is correct, then the hydroxylamine compounds, HA-SR, should not be stable and would decompose to the parent nitrone, ST, and thiol, RSH. In agreement with this hypothesis, the photolysis of the solutions of 10 mM GSNO or 10 mM AcSNO in the presence of 42.5 mM DEPMPO, with a UV lamp (15 mW/cm^2 intensity) at 500−600 nm over a time interval up to 90 min did not lead to the appearance of any new ^{31}P NMR signals (data not shown). The fraction of the decomposition of GSNO in this case was up to 90% (see Materials and Methods). Interestingly, 30 min of laser photolysis of the same solution at 532 nm, with higher irradiation

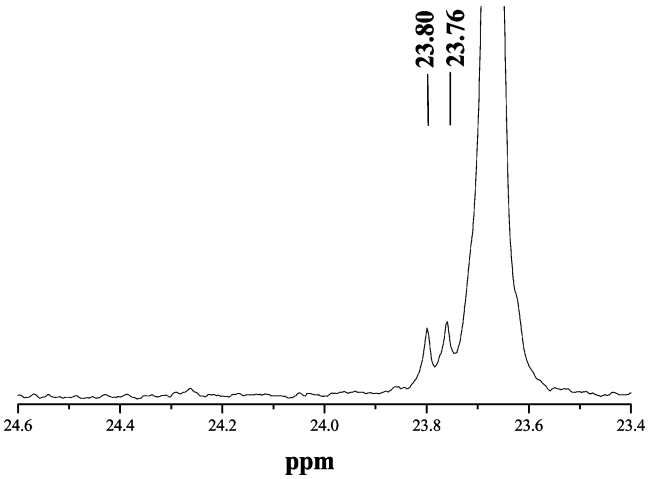

Figure 4. ^{31}P NMR spectrum of the mixture of 42.5 mM DMPO and 10 mM GSNO in 0.1 M phosphate buffer, pH 7.0, measured after irradiation by a Nd:YAG laser at 532 nm with intensity 30 mJ/cm^2 per pulse. The laser frequency was 25 Hz, and the irradiation time 30 min. Number of scans, 256; LB = 0.3. The estimated concentration of the product from the integral intensity of the new peaks at 23.80 and 23.76 ppm is equal to 2.2 ± 1 mM.

power of about 750 mW/cm^2 (30 mJ/pulse, frequency 25 Hz, irradiated area 1 cm^2) results in the appearance of two new products with ratio 1:1 at 23.80 and 23.76 ppm and a total concentration of 2.2 ± 1 mM (Figure 4). These values of chemical shift are characteristic for nitrone derivatives of DEPMPO.[15] Taking into account that both glutathione and DEPMPO structures have chiral centers, these products may be assigned to different diastereoisomers of the expected nitrone, N−SG. The observation of the signals assigned to the nitrone compounds, N−SG, exclusively at high irradiation power is consistent with the prevailing bimolecular decay of the paramagnetic adduct by reaction 4 at high initial concentration of ST/RS$^\bullet$. Meanwhile, it also opens a question about the origin of other pathways of the adduct degradation in our system that compete with bimolecular decay (4) at lower irradiation power. Note that kinetic analysis of the nitrone formation upon laser photolysis (see kinetic analysis section below) predicts nitrone accumulation of up to about 2.4 mM, which is in a good agreement with this experimental data.

EPR Studies of the Kinetics and Mechanism of the Decay of the Adducts of Nitrones with Thiyl Radicals. Figure 5 shows the kinetics of the decay of the glutathiyl radical with nitrone spin traps DMPO and DEPMPO. The kinetics was measured after various numbers of laser pulses of irradiation at 308 nm of the 0.1 M phosphate buffer solution, pH 7.0, containing 5 mM GSNO and 88.5 mM DMPO or 85 mM DEPMPO. As seen in Figure 5, the initial signal of the DMPO/GS$^\bullet$ and DEPMPO/GS$^\bullet$ adducts is proportional to the number of laser pulses and completely decays after 150 or 800 s, correspondingly. The photolysis of CySNO in the presence of the traps shows a similar qualitative picture, while quantitative analysis was impossible due to the limited stability of CySNO. The observed lifetime of DMPO thiyl radical adduct is somewhat lower than previously observed [17,21]. An explanation of the lifetime differences in various systems will be given after detailed analysis of the kinetic scheme.

Fitting DMPO/GS$^\bullet$ and DEPMPO/GS$^\bullet$ kinetics (Figure 5) with the first- or second-order decay curves does not provide satisfactory agreement with the experimental kinetics (results of this analysis not shown). Therefore, a combination of first-

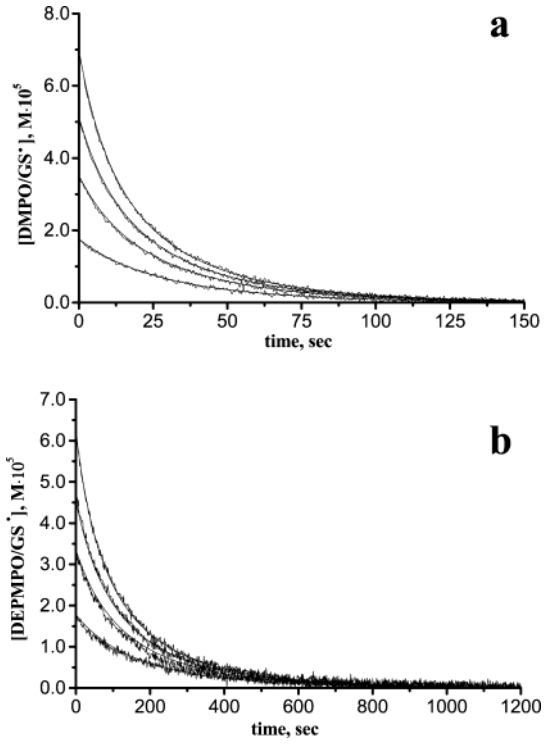

Figure 5. EPR kinetics decay measured after one, two, three, and four pulses of laser irradiation of the 0.1 M phosphate buffer, pH 7.0, 5 mM GSNO, and 88.5 mM DMPO (a) or 85 mM DEPMPO (b). The calculated kinetics is a nonlinear least-squares fit to the eq 6, yielding parameters $k_I = (3.1 \pm 0.4) \times 10^{-2}$ s^{-1} and $k_{II} = (7.9 \pm 2.0) \times 10^2$ M^{-1} s^{-1} (a) and $k_I = (4.1 \pm 0.2) \times 10^{-3}$ s^{-1} and $k_{II} = (1.0 \pm 0.3) \times 10^2$ M^{-1} s^{-1} (b).

and second-order decays was proposed, namely

$$\frac{d[ST/RS^\bullet]}{dt} = -k_I[ST/RS^\bullet] - k_{II}[ST/RS^\bullet]^2 \qquad (5)$$

where k_I and k_{II} are the observed rate constants of first- and second-order decay. The analytical solution of the eq 5 is given by eq 6

$$[ST/RS^\bullet] = \left[\left(\frac{1}{[ST/RS^\bullet]_0} + \frac{k_{II}}{k_I}\right)e^{k_I t} - \frac{k_{II}}{k_I}\right]^{-1} \qquad (6)$$

where $[ST/RS^\bullet]_0$ is the initial concentration of the radical adduct. The fitting of the eq 6 to the experimental data provides an excellent agreement of calculated and experimental kinetics, as shown by the filled curves in Figure 5. The second-order decay can be explained by the bimolecular disproportionation described by reaction 4. The origin of the monomolecular decay is somewhat more intriguing and was carefully elaborated on in the present work. The simplest explanation can be done by hypothesizing the reversibility of reaction 3, i.e., decomposition of the spin adduct back to parent nitrone and glutathiyl radical. The further analysis of the whole body of the kinetic studies is consistent with this hypothesis and is presented in a separate section. Nevertheless, the reversibility of the basic spin trapping reaction 3 is never discussed in the literature and requires direct experimental proof, particularly taking into account its far-reaching implications.

Direct Experimental Proof of the Reversibility of Spin Trapping of Glutathiyl Radicals by Nitrone Spin Traps. *1. The Formation of DEPMPO/GS$^\bullet$ Adduct during Decomposition of DMPO/GS$^\bullet$.* The reversibility of the spin trapping reaction 3

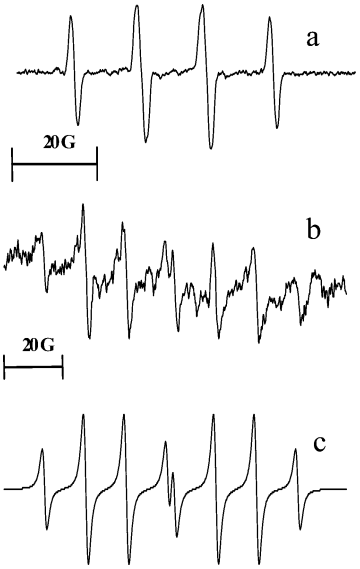

Figure 6. (a) EPR spectrum obtained during laser irradiation of the solution of DMPO and GSSG. First, 0.1 M GSSG and 88.5 mM DMPO were added to 0.1 M phosphate buffer. Then the solution was titrated to pH 7.0, bubbled by Ar during 15 min, and transferred to the EPR cell. The spectrum has been measured during laser irradiation at 308 nm. Number of scans, four. (b) A 2 mL sample of the same mixture as in part a was placed into the 1 cm quartz cell and irradiated by laser light with frequency 10 Hz during 20 s (~30 mJ per pulse). Immediately after that, 85 mM DEPMPO was added and the solution was transferred to the EPR flat cell. The spectrum was measured about 2 min after DEPMPO addition. The spectrometer settings were as follows: sweep width, 150 G; microwave power, 5 mW; modulation amplitude, 1 G; time constant, 81.92 ms; sweep time, 40 s; number of scans, four. (c). Simulated EPR spectrum with parameters $a_P = 45.81$ G, $a_N = 14.14$ G, and $a_H = 14.94$ G.

proposes release of glutathiyl radicals from the DMPO/GS$^\bullet$ adduct. Therefore, subsequent addition of the DEPMPO spin trap should result in the appearance of the DEPMPO/GS$^\bullet$ adduct. To test this hypothesis, we generated GS$^\bullet$ by the photolysis of disulfide GSSG. Figure 6a shows an EPR spectrum registered during laser photolysis of 0.1 M GSSG in the presence of 88.5 mM DMPO, which was assigned to DMPO/GS$^\bullet$ adduct based on the values of its hyperfine constants, $a_N = 15.12$ G and $a_H = 16.11$ G. In parallel experiments after irradiation was stopped, 42.5 mM DEPMPO was added to the solution, and the EPR spectrum was measured afterward (Figure 6b) with the parameters characteristic for DEPMPO/GS$^\bullet$ adduct ($a_P = 45.81$ G, $a_N = 14.14$ G, $a_H = 14.94$ G). The formation of DEPMPO/GS$^\bullet$ adduct after addition of DEPMPO to DMPO/GS$^\bullet$ indicates the presence of GS$^\bullet$ radical in the solution, although GS$^\bullet$ radicals are fully scavenged by 88.5 mM DMPO spin trap (rate constant, 2.6×10^8 M^{-1} s^{-1} [22]) in a less than 100 ns. Taking into account that DEPMPO/GS$^\bullet$ was not formed in the absence of photolysis (data not shown), it should be concluded that GS$^\bullet$ radical is generated directly from DMPO/GS$^\bullet$ radical adduct.

2. The Formation of $CO_2^{\bullet-}$ Radical from DMPO/GS$^\bullet$ in the Precence of Formate. Glutathiyl radical is able to abstract the hydrogen atom from formate ion with the rate constant $k_7 = 8 \times 10^5$M^{-1} s^{-1}:[23]

$$GS^\bullet + HCO_2^- \xrightarrow{k_7} GSH + CO_2^{\bullet-} \qquad (7)$$

On the basis of reaction 7, release of glutathiyl radicals from the DMPO/GS$^\bullet$ adduct in the presence of formate, $HCOO^-$, should lead to the formation of the carbonyl radical, $CO_2^{\bullet-}$, and, as a consequence, to the accumulation of comparatively

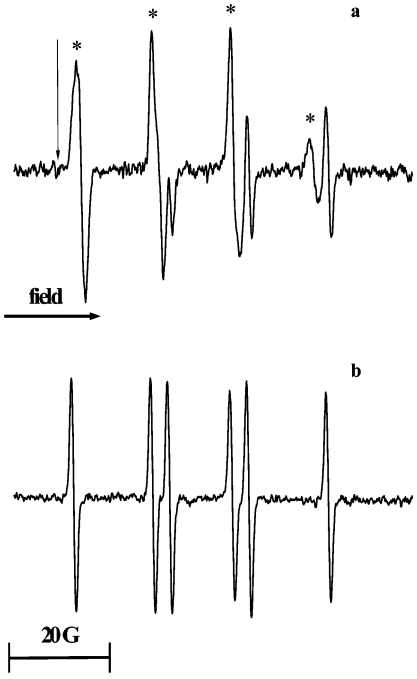

Figure 7. EPR spectra of the solution of DMPO, GSNO, and HCO_2Na in phosphate buffer measured after laser irradiation. First, 2 M HCO_2Na was added to 0.1 M phosphate buffer and the solution was titrated to pH 7.0. After that 5 mM GSNO and 88.5 mM DMPO were added. The spectrometer settings were as follows: sweep width, 80 G; modulation amplitude, 1 G; time constant, 81.92 ms; microwave power, 5.19 mW, sweep time, 41.94 s. (a) Spectrum measured immediately after laser irradiation (four pulses × 30 mJ), one scan; an arrow indicates the moment of irradiation; the peaks of DMPO/GS$^\bullet$ adduct are marked by an asterisk. (b) Spectrum measured 2 min later, eight scans. The hyperfine constants determined by simulation of the spectrum are $a_N = 15.7$ G and $a_H = 19.0$ G, in good agreement with published data for the DMPO/$CO_2^{\bullet-}$ adduct.[24]

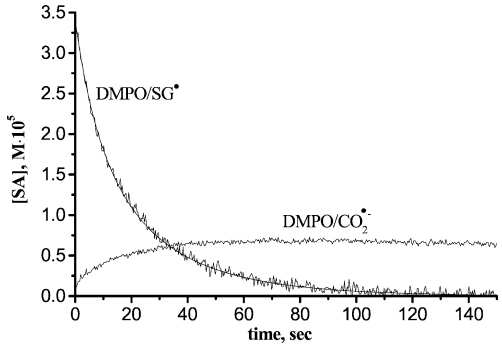

Figure 8. Time evolution of the DMPO spin adducts concentration, [SA], measured from EPR signal intensity changes after GSNO photolysis in the presence of sodium formate. First 2 M HCO_2Na was added to the 0.1 M phosphate buffer, and the solution was titrated to pH 7.0. After that 5 mM GSNO and 88.5 mM DMPO were added. The mixture was bubbled by Ar during 30 min and transferred to the EPR cavity. The kinetics of DMPO/GS$^\bullet$ and DMPO/$CO_2^{\bullet-}$ adducts were registered using corresponding high field spectral components (see Figure 7). The calculated kinetics of DMPO/GS$^\bullet$ decay is a nonlinear least-squares fit to eq 6, yielding parameters $k_I = (3.2 \pm 0.4) \times 10^{-2}$ s^{-1} and $k_{II} = (1.2 \pm 0.3) \times 10^3$ M^{-1} s^{-1}.

stable DMPO/$CO_2^{\bullet-}$ radical adduct. In agreement with this hypothesis, the photolysis of 5 mM GSNO in Ar-bubbled 0.1 M phosphate buffer in the presence of 88.5 mM DMPO and 2 M sodium formate (Figures 7 and 8) resulted in the decay of DMPO/GS$^\bullet$ adduct with corresponding accumulation of DMPO/$CO_2^{\bullet-}$ adduct. EPR spectrum shown in Figure 7a was registered immediately after laser irradiation (four pulses × 30 mJ) and

consists of signals from the both radical adducts. The DMPO/GS$^\bullet$ adduct completely disappeared within 2 min with parallel accumulation of the EPR signal of DMPO/$CO_2^{\bullet-}$ adduct (Figure 7b). Figure 8 demonstrates the experimental kinetics measured immediately after laser irradiation. It should be noted that under the experimental concentrations of the spin trap and formate, GS$^\bullet$ radical initially formed under photolysis is predominantly scavenged by DMPO (rate constant 2.6×10^8 M^{-1} s^{-1} [22]) rather than reacting with formate by reaction 7 ($k_7 = 8 \times 10^5$ M^{-1} s^{-1} [23]), in agreement with experimental data (Figure 7a). The release of GS$^\bullet$ radical from DMPO/GS$^\bullet$ adduct results in establishment of quasistationary level of GS$^\bullet$, which reacts with formate, forming carbonyl radical, with subsequent accumulation of DMPO/$CO_2^{\bullet-}$ adduct (Figure 7b and 8). Fitting the kinetics of the DMPO/GS$^\bullet$ decay shown in Figure 8 allows good agreement between calculated and experimental dependences, with the rate constant of monomolecular decomposition being equal to 0.03 s^{-1} (see next section for details).

Kinetic Analysis of Laser Photolysis of GSNO Solution in the Presence of the Nitrones. *1. Kinetic Scheme and Decay of ST/GS$^\bullet$ Adduct.* To quantitatively describe the kinetics of the decay of the nitrone adducts with glutathiyl radical, ST/GS$^\bullet$, formed due to photolysis of GSNO (Figure 5), the following reactions should be considered:

$$\text{GSNO} \xrightarrow{h\nu} \text{GS}^\bullet + \text{NO}^\bullet \quad (8)$$

$$\text{GS}^\bullet + \text{ST} \leftrightarrow \text{ST/GS}^\bullet \quad (9)$$

$$\text{GS}^\bullet + \text{DMPO} \leftrightarrow \text{DMPO/GS}^\bullet \quad k_{9a} = 2.6 \times 10^8\ M^{-1}\ s^{-1}\ [22]$$

$$k_{-9a} = 0.3\ s^{-1}\ \text{(this work)} \quad (9a)$$

$$\text{GS}^\bullet + \text{DEPMPO} \leftrightarrow \text{DEPMPO/GS}^\bullet$$

$$k_{9b} = 1.5 \times 10^8\ M^{-1}\ s^{-1}$$

$$k_{-9b} = 0.02\ s^{-1}\ \text{(this work)} \quad (9b)$$

$$2(\text{ST/GS}^\bullet) \rightarrow \text{bimolecular decay} \quad (10)$$

$$2(\text{DMPO/GS}^\bullet) \rightarrow \text{bimolecular decay}$$

$$k_{10a} = 4 \times 10^2\ M^{-1}\ s^{-1}\ \text{(this work)} \quad (10a)$$

$$2(\text{DEPMPO/}GS^\bullet) \rightarrow \text{bimolecular decay}$$

$$k_{10b} = 0.5 \times 10^2\ M^{-1}\ s^{-1}\ \text{(this work)} \quad (10b)$$

$$\text{GS}^\bullet + \text{GSNO} \rightarrow \text{GSSG} + \text{NO}^\bullet \quad k_{11} = 1.7 \times 10^9\ M^{-1}\ s^{-1}\ [18]$$

$$k_{11} = (6.1 \pm 1.5) \times 10^8\ M^{-1}\ s^{-1}\ \text{(this work)} \quad (11)$$

$$2\text{GS}^\bullet \rightarrow \text{GSSG} \quad k_{12} = 1.5 \times 10^9\ M^{-1}\ s^{-1}\ [23] \quad (12)$$

$$\text{GS}^\bullet + \text{NO}^\bullet \rightarrow \text{GSNO} \quad \text{ref 20} \quad (13)$$

$$\text{GS}^\bullet + \text{O}_2 \rightarrow \text{GSOO}^\bullet \quad k_{15} = 2 \times 10^9\ M^{-1}\ s^{-1}\ [25] \quad (14)$$

Reaction 9 is shown as reversible to account for the experimentally observed GS$^\bullet$ radical release from the ST/GS$^\bullet$ adduct. This release results in establishment of a quasistationary concentration of GS$^\bullet$ radical, which decays also in reactions 11−14. Among the latter reactions, only reaction 11 can significantly contribute to GS$^\bullet$ decay by mechanisms other than spin-trapping reaction under our experimental conditions. The insignificant difference between the kinetics of DMPO/GS$^\bullet$ decay measured upon GSNO photolysis in air-saturated and argon-bubbled solutions (data not shown, see Materials and Methods) is consistent with the negligible role of reaction 14 upon experimentally used high concentrations of the spin trap. The performed numerical calculations showed that the contribution of the reactions 12 and 13, being of second-order on the concentration of generated radical species, is negligible even for diffusion-controlled reactions and may become significant only at bimolecular rate constants being larger than 10^{12} M^{-1} s^{-1}. In agreement with this statement, NO significantly decreased the lifetime of the radical adduct only at concentrations one order larger compared with those formed in our experiments (data not shown).

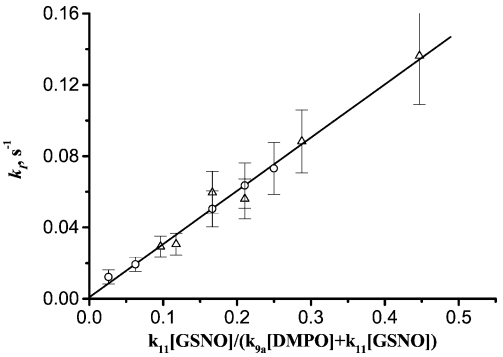

Figure 9. Dependence of the k_I value on the term k_{11}[GSNO]/(k_{9a}[DMPO] + k_{11}[GSNO]). The experiments were done in air-saturated 0.1 M phosphate buffer, pH 7.0, containing GSNO and DMPO. Kinetic decay was registered after irradiation of the solution by one, two, three, and four laser pulses. Obtained kinetics with different radical adduct concentrations (as in Figure 5) were fitted using eq 6 with fitting parameters k_I and k_{II}. (○) Variation of GSNO concentration at [DMPO] = 88.5 mM; (△) variation of DMPO concentration at [GSNO] = 5 mM. Note that the value of $k_{11} = (6.1 \pm 1.5) \times 10^8$ M^{-1} s^{-1} measured in this work (see laser flash photolysis section) was used in calculations.

The consideration of reactions 9−11 using the approximation of the quasistationary concentration for [GS$^\bullet$] gives the following solution for spin adduct decay:

$$\frac{d[\text{ST/GS}^\bullet]}{dt} = -k_{-9}\frac{k_{11}[\text{GSNO}]}{k_9[\text{ST}] + k_{11}[\text{GSNO}]}[\text{ST/GS}^\bullet] - 2k_{10}[\text{ST/GS}^\bullet]^2 \quad (15)$$

Equation 15 coinsides with eq 5, which describes the experimental kinetics, assuming

$$[\text{ST/RS}^\bullet] = [\text{ST/GS}^\bullet],\ k_I = k_{-9}\frac{k_{11}[\text{GSNO}]}{k_9[\text{ST}] + k_{11}[\text{GSNO}]},\ \text{and}\ k_{II} = 2k_{10} \quad (16)$$

where k_i and k_{-i} are the rate constant of forward and reverse reaction i, correspondingly.

Figure 9 demonstrates that the dependence of k_I on the term k_{11}[GSNO]/(k_{9a}[DMPO] + k_{11}[GSNO]) for DMPO allows excellent linear approximation, namely

$$k_I(s^{-1}) = (0.30 \pm 0.01)\frac{k_{11}[\text{GSNO}]}{k_{9a}[\text{DMPO}] + k_{11}[\text{GSNO}]} \pm 0.0027 \quad (17)$$

Therefore, according to eqs 16 and 17 the rate constant for the decomposition of the DMPO/GS$^\bullet$ adduct, k_{-9a}, is equal to (0.30 ± 0.01) s^{-1}. As for bimolecular decay, we did not observe any dependence of the observed rate constant k_{II} on the concentra-

tions of [GSNO] and [DMPO], in agreement with eq 16. The k_{10a} value was found to be equal to $(4.0 \pm 1.0) \times 10^2$ M^{-1} s^{-1}.

As we mentioned above, the degradation of the DEPMPO/GS• adduct (Figure 5b) also is described by first- and second-order decay with $k_I = (4.1 \pm 0.2) \times 10^{-3}$ s^{-1} and $k_{II} = (1.0 \pm 0.3) \times 10^2$ M^{-1} s^{-1} (see Figure 5 caption). Applying similar arguments to the analysis of these kinetics, based on the reactions 9−11, and therefore using eq 16, we obtain the rate constant for the monomolecular decomposition of DEPMPO/GS• adduct, $k_{-9b} = (2.1 \pm 0.1) \times 10^{-2}$ s^{-1}, and the rate constant for its bimolecular decay, $k_{10b} = (50 \pm 15)$ M^{-1} s^{-1}. The calculation of the value of k_{-9b} requires knowledge of the rate constant k_{9b} for the direct reaction of GS• trapping by DEPMPO. In the present paper we have measured this constant by laser flash photolysis and found it to be equal to 1.5×10^8 M^{-1} s^{-1} (see laser flash photolysis section).

2. Kinetics of Accumulation of DMPO/$CO_2^{\bullet-}$ Adduct in the Presence of Formate. In the presence of formate, an additional pathway of GS• decay by reaction 7 must be considered. Again, using a quasistationary approximation for the concentration of GS• radical, we obtain the following equations for DMPO/GS• adduct decay:

$$\frac{d[DMPO/GS^\bullet]}{dt} = -\left(k_{-9a}\frac{k_{11}[GSNO] + k_7[HCO_2^-]}{k_{9a}[ST] + k_{11}[GSNO] + k_7[HCO_2^-]}\right)[DMPO/GS^\bullet] - 2k_{10a}[DMPO/GS^\bullet]^2 \quad (18)$$

Equation 18 formally coincides with the eq 5. Therefore, the decay of DMPO/GS• adduct is described by eq 6 with the parameters

$$[ST/RS^\bullet] = [DMPO/GS^\bullet],\ k_I = k_{-9a}\frac{k_{11}[GSNO] + k_7[HCO_2^-]}{k_{9a}[ST] + k_{11}[GSNO] + k_7[HCO_2^-]},\ \text{and}\ k_{II} = 2k_{10a} \quad (19)$$

A good agreement between calculated and experimental kinetics (Figure 8) has been observed for the decay of DMPO/GS• adduct using known values of the rate constants and yielding fitting parameters $k_{-9a} = (0.2 \pm 0.05)$ s^{-1} and $k_{10a} = (600 \pm 150)$ M^{-1} s^{-1}. These values of k_{-9a} and k_{10a} are in a reasonable agreement with those obtained in the absence of formate (Figure 5a), particularly taking into account some uncertainty in the value of k_7[16,23] and appearance of an additional pathway of bimolecular decomposition between DMPO/GS• and DMPO/$CO_2^{\bullet-}$ adducts.

An accumulation of DMPO/$CO_2^{\bullet-}$ adduct, in its turn, is described by the following equation upon the assumptions that (i) $CO_2^{\bullet-}$ radical generated by reaction 7 is completely trapped by DMPO and (ii) the formed DMPO/$CO_2^{\bullet-}$ adduct insignificantly decays for the experimental time:

$$\frac{d[DMPO/CO_2^{\bullet-}]}{dt} = k_{-9a}\frac{k_7[HCO_2^-]}{k_{9a}[ST] + k_{11}[GSNO] + k_7[HCO_2^-]}[DMPO/GS^\bullet] = k_{III}[DMPO/GS^\bullet] \quad (20)$$

The analytical solution of this equation can be obtained after substitution of the [DMPO/GS•] (eq 6 with parameters in eq 19), namely

$$[DMPO/CO_2^{\bullet-}] = \frac{k_{III}}{k_{II}}\left(-k_I + \ln\left(\left(\frac{k_{II}}{k_I}[DMPO/GS^\bullet]_0 + 1\right) \times \exp(k_I t) - \frac{k_{II}}{k_I}[DMPO/GS^\bullet]_0\right)\right) \quad (21)$$

where $[DMPO/GS^\bullet]_0$ is the initial concentration of the DMPO/GS• adduct. Equation 21 qualitatively describes the experimentally observed accumulation of DMPO/$CO_2^{\bullet-}$ adduct. The following expression can be obtained for the maximal value of the concentration of the DMPO/$CO_2^{\bullet-}$ adduct that can be accumulated in the absence of its decay:

$$[DMPO/CO_2^{\bullet-}]_{max} = \frac{k_{III}}{k_{II}}\ln\left(\frac{k_{II}}{k_I}[DMPO/GS^\bullet]_0 + 1\right) \quad (22)$$

Using the obtained values of k_{-9a} and k_{10a} and published values of the rate constants k_7, k_{9a}, and k_{11} we estimated expression 22 to be equal to 1.1×10^{-5} M, in reasonable agreement with the experimental value 0.72×10^{-5} M. Note that quantitative description of the kinetics of accumulation of DMPO/$CO_2^{\bullet-}$ adduct requires knowledge of the mechanism of its decay, which was not a subject of this study.

Therefore, the kinetic analysis of the experimental data support the existence of monomolecular decomposition of the adduct of nitrones with glutathiyl radicals, ST/GS•, with recycling of the parent nitrone and GS• radical.

3. Accumulation of DEPMPO−SG Nitrone upon GSNO Photolysis. Bimolecular disproportionation of the DEPMPO/GS• adduct results in formation of the nitrone DEPMPO−SG, according to reaction 4. The efficiency of this process is determined by the ratio of radical adduct degradation in the first- and second-order reactions, namely by the factor, k_{II}[DEPMPO/GS•]/k_I (see eqs 5 and 16), and therefore by the rate, I, of GS• generation upon continuous photolysis. The value of I that will result in equal efficiency of mono- and bimolecular decay was estimated as 4 μmol/L/s for the experimentally used concentrations of DEPMPO and GSNO (42.5 and 10 mM, correspondingly), assuming steady-state approximation for [DEPMPO/GS•] and [GS•] and using the rate constants obtained in the previous sections. The initial value of I in the case of UV lamp photolysis was estimated to be significantly lower, about 0.2 μmol/L/s (average extinction coefficient, $\epsilon_{GSNO} \approx 7$ M^{-1} s^{-1}, in the range 500−600 nm, and quantum yield about 0.026[17]). In the case of laser photolysis (see Materials and Methods), this value was estimated to be about 6.7 μmol/L/s, which should result in 2.4 mM accumulation of the nitrone DEPMPO−SG, in fairly good agreement with the experimentally observed value (Figure 4).

Laser Flash Photolysis Studies of the Reaction of GS• Radical with DEPMPO and GSNO. The rate constants of GS• addition to GSNO, k_{11}, and to DEPMPO, k_{9b}, were calculated from the measurements of the decay of GS• radical monitored at 350 nm using the laser flash photolysis setup described in the Materials and Methods. The absorption signal decayed exponentially upon the photolysis of 0.4−1.6 mM GSNO solutions. The observed pseudo-first-order rate constant linearly depends on the initial GSNO concentration, in agreement with reaction 11, giving $k_{11} = (6.1 \pm 1.5) \times 10^8$ M^{-1} s^{-1}.

The measurement of the rate constant k_{9b} of the reaction of GS• with DEPMPO was performed by irradiation of 1 mM GSNO solution in the presence of DEPMPO; the concentration

of DEPMPO varied from 2.84 to 11.35 mM. The absorption signal decayed exponentially, and the value k_{9b} was calculated from the obtained linear dependence of the observed pseudo-first-order rate constant on the term k_{9b}[DEPMPO] + k_{11}[GSNO], yielding $k_{9b} = (1.5 \pm 0.3) \times 10^8$ M^{-1} s^{-1}.

Discussion

The chemistry of nitrones is of significant interest, due to their wide applications as spin traps for EPR detection of short-lived radical intermediates in biological systems[1,2] and growing applications as therapeutic agents.[3,4] An observation of the new reactions of nitrones with (bi)sulfite and thiols may be of critical importance for the understanding of their biological activities. Indeed, the reverse reaction of nucleophilic addition of thiols to the nitrones provides the unique mechanism of the detoxification of thiyl radicals. Thiols, being primary antioxidants in vivo, form thiyl radicals during their antioxidant activity. In turn, nitrones may recycle thiol antioxidants by trapping the thiyl radicals and releasing the thiols after the reduction of the paramagnetic adduct by biologically relevant reductants, such as ascorbate. The knowledge of these new reactions of nitrones can assist investigators in avoiding erroneous interpretation of spin-trapping experiments. The reversible nucleophilic addition of both thiols and thiyl radicals to the nitrones may significantly affect not only the quantitative analysis of the data but even the conclusion about the origin of the paramagnetic adduct.

The potential for nucleophilic addition to nitrones has been known for a long time.[26] For example, Bonnet at al.[27] described the irreversible addition of C-centered anions (Grignard reagents, hydrogen cyanide) to a variety of nitrones with formation of isolatable hydroxylamine derivatives. Nucleophilic addition reactions of O-centered anions ($^-$OH, $^-$OCH$_3$)[28,29] to DMPO and of the anion of H_2O_2 to 4-POBN[30] are also described. Alberti et al.[31] showed the nucleophilic addition of a range of heterocyclic N−H bases toward PBN and DMPO. Forrester and Hepburn[32] discussed the nucleophilic addition of a numbers of anions (of nitromethane, phthalamide, hydrogen and benzyl cyanide, and acetate) to PBN with formation of the hydroxylamine derivatives followed by their oxidation to EPR-detectable nitroxides. This artificial pathway of paramagnetic adduct formation was named after this work, i.e., the Forrester−Hepburn mechanism, and must be a matter of great concern in interpretation of spin-trapping experiments. There are numerous reports on the involvement of the Forrester−Hepburn mechanism in the formation of EPR-detectable adducts of spin traps[33−38] (see also refs 39 and 40 for reviews).

In a common case, addition of negatively charged nucleophile, Nu^-, to a nitrone, ST, can be described by the following generalized equations:

$$\mathrm{NuH} \overset{K_{\mathrm{NuH}}}{\longleftrightarrow} \mathrm{Nu}^- + \mathrm{H}^+ \tag{23}$$

$$\mathrm{Nu}^- + \mathrm{ST} \overset{K_{\mathrm{ad}}}{\longleftrightarrow} \mathrm{ST}^-\mathrm{Nu} \tag{24}$$

$$\mathrm{ST}^-\mathrm{Nu} + \mathrm{H}^+ \overset{K_{\mathrm{b}}}{\longleftrightarrow} \mathrm{ST(H)Nu} \tag{25}$$

where ST(H)Nu and ST^-Nu are the corresponding hydroxylamine and its deprotonated form. The acidity of hydrohylamines in water is supposed to be similar to that for aliphatic alcohols, p$K_a \approx 16-18$; e.g. the acidity of *N*-phenylhydroxylamine, PBN, is similar to that for isopropyl alcohol, p$K = 17.1$.[41] Therefore, at neutral pH at equilibrium, reaction 25 is strongly shifted to the right, and the ratio of finally formed hydroxylamine to initially available nitrone is determined by equilibrium constants K_{NuH}, K_{ad}, and K_{b} of the reactions 23−25 and by the equilibrium concentrations of the NuH at given pH, namely

$$[\mathrm{ST(H)Nu}]/[\mathrm{ST}] = K_{\mathrm{NuH}}K_{\mathrm{ad}}K_{\mathrm{b}}[\mathrm{NuH}] \tag{26}$$

Table 1 represents several S-centered nucleophiles, their p$K = -\log K_{\mathrm{NuH}}$ values, and estimates of the product $K_p = K_{\mathrm{NuH}}K_{\mathrm{ad}}K_{\mathrm{b}}$. The strong pH dependence of the equilibrium hydroxylamine concentration has been observed for (bi)sulfite addition toward DMPO and DEPMPO, in agreement with eqs 23 and 26.[5,6] For the other nucleophiles shown in Table 1, the pH dependence is leveled at neutral pH (p$K_{\mathrm{NuH}} \gg$ pH, resulting in [NuH] ≫ [Nu^-]). A thousand times difference in K_p value for the reaction of DEPMPO with nucleophiles of the same charge, SO_3^{2-} and $^-SCH_2COO^-$, correlates with the difference in their pK_{NuH} (ΔpK ≈ 3). Also the lower value of K_p for the reaction of DEPMPO with GSH (undetectable in our experiments) compared with that for CySH may be related to higher pK value of GSH.

The further oxidation of the hydroxylamines results in the formation of the corresponding radical adduct with sulfite radical anion or with the thiyl radicals, exemplifying nonconventional formation of the paramagnetic adduct by the Forrester−Hepburn[32] mechanism. The hydroxylamines have low redox potentials, their anodic half-wave redox potentials, $E_{1/2}$, being in the range of −(0.4−0.5) V vs SCE in aqueous solution for a series of alkyl and arylhydroxylamines in their anionic form and 0.5−0.8 V in acetonitrile in their neutral form.[39,42−44] Therefore, they can be oxidized even by weak oxidants such as dioxygen ($E°$ ($O_2/O_2^{\bullet-}$)= −0.4 V in water) or by a wide range of redox proteins in biological systems. Taking into account that redox potentials of sulfite and thiols are normally in the same range or higher (0.4 V for $SO_3^{\bullet-}/SO_3^{2-}$, 0.6 V for $SO_3^{\bullet-}/HSO_3^-$,[45] and 0.7 V for $CyS^{\bullet}$/CySH[46]), one has to unambiguously consider the possibility of paramagnetic adduct formation from nitrones in the presence of thiols and oxidants via the Forrester−Hepburn mechanism, i.e., reactions 23−25 followed by hydroxylamine oxidation. The oxidation of hydroxylamine in the presence of oxygen will result in superoxide generation, followed by its own chemistry, therefore adding complexity to the system. Note that equilibrium concentrations of hydroxylamine formed are sufficient to explain a significant rate of accumulation of the paramagnetic adduct in the presence of the spin trap, nucleophile, and oxidant. At 1 mM concentration of nucleophile and 50 mM of spin trap, it corresponds, according to eq 26 with K_p given in Table 1, to concentrations of hydroxylamine derivative ST(H)Nu in amounts about 0.9 mM (NuH = HSO_3^-), 7 μM (NuH = $HSCH_2COO^-$), 1.5 μM (NuH = CySH), and <0.1 μM (NuH = GSH).

If nucleophilic addition to nitrones, in our opinion, were not sufficiently taken into consideration, particularly in spin-trapping experiments, there would be even less noticed about its reversibility. Meanwhile, the reverse reaction is worth considering for a variety of reasons. First, it shows that the product of nucleophilic addition to the nitrones may be important in a reaction mixture while it would not be isolated as an individual substance. The drastic example is sulfite addition to nitrones with mM (!) product formation. Second, the reversibility of reaction 24 provides a unique mechanism for the detoxification of reactive radicals, $Nu^{\bullet}$, by nitrones:

$$\mathrm{Nu}^{\bullet} + \mathrm{ST} \rightarrow \mathrm{ST}^{\bullet}\mathrm{Nu} \tag{27}$$

$$\mathrm{ST}^{\bullet}\mathrm{Nu} \xrightarrow{\text{Reduction}} \mathrm{ST(H)Nu} \tag{28}$$

$$\mathrm{ST(H)Nu} \rightleftarrows \mathrm{ST} + \mathrm{NuH} \tag{29}$$

This mechanism seems to be particularly important for thiols, NuH = RSH, widely considered as a primary antioxidant. Reaction 29, being thermodynamically equivalent to the sum of reactions 24 and 25, essentially explains our failure to accumulate ST(H)−SG adduct, even at very high rates of GS• generation by laser photolysis of nitrosoglutathione. The only adduct we were able to detect was assigned to DEPMPO−SG nitrone on the basis of the ^{31}P NMR shift. Interestingly, also only one diamagnetic product of degradation of the DMPO/GS• adduct was measured using HPLC by Stoyanovsky et al.[47] and assigned to the DMPO−SG nitrone. These data are in agreement with our report on reverse reaction 29 for DEPMPO/OH and DEPMPO/OOH hydroxylamines that prevented us from accumulating these diamagnetic products upon generation of OH• and $O_2^{\bullet-}$ radicals.[15,48]

The attempts to accumulate hydroxylamine derivatives of DEPMPO adduct during photochemical generation of RS• encouraged us to look into the details of the DEPMPO/GS• and DMPO/GS• decays. The kinetics showed superposition of first- and second-order decays that is quite typical for the spin adduct degradation.[49,50] Normally second-order decay is observed only at high concentrations of generated adduct in comparatively pure chemical systems,[15,49] while first-order decay dominates at low adduct concentrations in various biological systems.[51] The mechanism of second-order decay for most cases is believed to be bimolecular disproportionation, as shown by eq 4 for thiyl radical adduct. The mechanisms of first-order decay vary depending on the sample composition and the presence of reducing agents. Nevertheless, it is a recognized intrinsic instability of the spin adducts of nitrones with the most biologically relevant radicals, e.g. superoxide, thiyl, and peroxyl radicals. The mechanisms for the self-degradation of these adducts may include several pathways but are far from understood. In the present work we have demonstrated degradation of the glutathiyl radical adducts with the nitrones DMPO and DEPMPO via the reverse spin-trapping reaction 9. The release of GS• radical from the DMPO/GS• adduct has been unambiguously proved by its further competitive reactions with another nitrone or with formate (Figures 6−8). The proposed kinetic scheme (reactions 7−11) allows quantitative description of all the observed kinetics. The reciprocal proportionality of the pseudo-first-order decay rate constant, k_I, to the concentration of spin trap and its direct proportionality to the concentration of the competitive reagent for GS• (GSNO, eq 16, or HCO_2^-, eq 18) are in excellent agreement with this scheme (see Figure 9). The rate constant of the GS• release from DMPO and DEPMPO, k_{-9}, was found to be equal to 0.3 and 0.02 s^{-1}, correspondingly. Note that the characteristic lifetime of the adducts strongly depends on the competitive reagent ($1/\tau = k_I$, eqs 16 and 18), explaining its significant variations in the different experimental conditions (refs 17 and 21 and this work). On the other hand, the ratio of the constants, showing about 15 times greater stability of the DEPMPO/GS• adduct compared with that for DMPO/GS• toward this mechanism of degradation, reflects intrinsic properties of the trap and does not depend on the sample composition.

The reversibility of spin trapping reaction, to our knowledge, has never been discussed in the literature. Nevertheless, the analogous breakdown of the series of 3-imidazoline-3-oxide nitroxides with formation of dinitrone 4*H*-imidazole di-*N*-oxides was previously described.[52,53] In another report, Karoui et al.[16] explained a time-dependent decrease in DEPMPO/GS• adduct with a parallel increase in DEPMPO/$CO_2^{\bullet}$ adduct upon the photolysis of GSNO, by the formation of $CO_2^{\bullet-}$ radical in the reaction (7) of formate with GS•. The simple kinetic estimates show that in the presence of 20 mM DEPMPO and 400 mM formate, the latter reaction can hardly compete with GS• scavenging by DEPMPO (the ratio $k_7[HCOO^-]/k_{9b}[DEPMPO] \approx 1.3 \times 10^{-3}$ if $k_7 = 10^4$ M^{-1} s^{-1},[16] or it is ≈0.1 if $k_7 = 8 \times 10^5$ M^{-1} s^{-1} [23]). These data are in agreement with our observation (Figure 8) and can be easily explained by establishment of a quasistationary concentration of GS• due to the reversibility of reaction 9. The reversibility of the spin-trapping reactions with the radicals beyond GS•, if they exist, may significantly influence the lifetime of the radical adducts and even facilitate the formation of new products. The probable role of the reverse spin trapping reaction in degradation of nitrone adducts with peroxyl and superoxide radicals is worth consideration. For example, the conversion of DMPO/−OOH to DMPO/−OH[54] with formation of −OH• radical,[55] the mechanism for which has been debated for many years, and the accumulation of carbon-centered adducts of DEPMPO upon superoxide generation[51] may be well related to this intrinsic instability of the superoxide adduct. Note also the difference of about 15 times in the lifetimes of superoxide adducts with DEPMPO and DMPO[49−51,56] This is in striking coincidence with 15 times lower rate constant of the reverse reaction 9 for DEPMPO/GS• adduct compared with that for DMPO/GS•. Moreover, the theoretically calculated energy difference between spin trap, ST, and its adduct with superoxide, ST/$O_2^{\bullet-}$, for the series of nitrones correlates well with the lifetime of the adducts,[50] further supporting a possible contribution of their breakdown through the reverse spin-trapping reaction.

In conclusion, we provide strong evidence for the importance of the reversible reaction of thiols and thiyl radicals with nitrone spin traps. We propose that the observations described here represent a fundamental chemical behavior that applies to a variety of redox reactions with nitrone spin traps that must be considered relevant.

Acknowledgment. This work was supported by grants from NHLB 53333, the Russian Foundation for Basic Research grants 02-04-48374 and 03-04-06189, and Ministry of Education of RF grant A03-2.11-822.

References and Notes

(1) Mason, R. P.; Hanna, P. M.; Burkitt, M. J.; Kadiiska, M. B. *Environ. Health Perspect.* **1994**, *102*, 33−36.

(2) Khan, N.; Swartz, H. *Mol. Cell. Biochem.* **2002**, *234−235*, 341−357.

(3) Floyd, R. A.; Hensley, K.; Forster, M. J.; Kelleher-Andersson, J. A.; Wood, P. L. *Mech. Aging Dev.* **2002**, *123*, 1021−1031.

(4) Kotake, Y. *Antioxid. Redox Signal.* **1999**, *1*, 481−499.

(5) Potapenko, D. I.; Bagryanskaya, E. G.; Reznikov, V. V.; Clanton, T. L.; Khramtsov, V. V. *Magn. Reson. Chem.* **2003**, *41*, 603−608.

(6) Potapenko, D. I.; Clanton, T. L.; Bagryanskaya, E. G.; Gritsan, N. P.; Reznikov, V. A.; Khramtsov, V. V. *Free Radic. Biol. Med.* **2003**, *34*, 196−206.

(7) Bryson, P. D. Sulfites and monosodium glutamate. In *Comprehensive Review in Toxicology for Emergency Clinicians*; Taylor & Francis: Washington, D.C., 1996; pp 697−703.

(8) Bush, R. K.; Taylor, S. L.; Busse, W. *J. Allergy Clin. Immunol.* **1986**, *78*, 191−202.

(9) Gunnison, A. F.; Jacobsen, D. W. Sulfite hypersensitivity. A critical review. In *CRC Critical Review in Toxicology*; CRC Press: Boca Raton, FL, 1987; pp 185−214.

(10) Pietraforte, D.; Mallozzi, C.; Scorza, G.; Minetti, M. *Biochemistry* **1995**, *34*, 7177−7185.

(11) Hart, T. W. *Tetrahedron Lett.* **1985**, *26*, 2013−2016.

(12) Glasoe, P. K.; Long, F. A. *J. Phys. Chem.* **1960**, *64*, 188−190.

(13) Molokov, I. F.; Tsentalovich, Yu. P.; Yurkovskaya, A. V.; Sagdeev, R. Z. *Photochem. Photobiol. A: Chem.* **1997**, *110*, 159−165.

(14) Tsentalovich, Yu. P.; Kulik, L. V.; Gritsan, N. P.; Yurkovskaya, A. V. *J. Phys. Chem. A.* **1998**, *102*, 7975−7980.

(15) Khramtsov, V.; Berliner, L. J.; Clanton, T. L. *Magn. Reson. Med.* **1999**, *42*, 228−234.
(16) Karoui, H.; Hogg, N.; Frejaville, C.; Tordo, P.; Kalyanaraman, B. *J. Biol. Chem.* **1996**, *271*, 6000−6009.
(17) Singh, R. J.; Hogg, N.; Joseph, J.; Kalyanaraman, B. *FEBS Lett.* **1995**, *360*, 47−51.
(18) Wood, P. D.; Mutus, B.; Redmond, R. D. *Photochem. Photobiol.* **1996**, *64*, 518−524.
(19) Barrett, J.; Debenham, D. F.; Glauser, J. *Chem. Commun.* **1965**, 248−249.
(20) Pou, S.; Rosen, G. M. *J. Chem. Soc., Perkin Trans. 2* **1998**, 1507−1512.
(21) Shi, X.; Dong, Z.; Dalal, N. S.; Gannett, P. M. *Biochim. Biophys. Acta* **1994**, *1226*, 65−72.
(22) Davies, M. J.; Forni, L. G.; Shuter, S. L. *Chem.-Biol. Interact.* **1987**, *61*, 177−188.
(23) Wardman, P. Reactions of Thiyl Radicals. In *Biothiols in Health and Disease*; Packer L, Cadenas E, Eds.; Marcel Dekker: New York, Basel, Hong Kong, 1995; pp 1−19.
(24) Mottley, C.; Mason, R. P. *Arch. Biochem. Biophys.* **1988**, *267*, 681−689.
(25) Tamba, M.; Simone, G.; Quintiliani, M. *J. Radiat. Biol.* **1986**, *150*, 595−600.
(26) Breuer, E. Nitrones and nitronic acid derivatives: Their structure and their role in synthesis. In *Nitrones, Nitronates and Nitroxides*; Patai S, Rappoport Z, Eds.; John Wiley & Sons: New York, 1989; pp 139−244.
(27) Bonnet, R.; Brown, R. F. C.; Clark, V. M.; Sutherland, I. O.; Todd, A. *J. Chem. Soc.* **1959**, 2094−2102.
(28) Makino, K.; Hagiwara, T.; Hagi, A.; Nishi, M.; Murakami, A. *Biochem. Biophys. Res. Commun.* **1990**, *172*, 1073−1080.
(29) Hanna, P. M.; Chamulitrat, W.; Mason, R. P. *Arch. Biochem. Biophys.* **1992**, *296*, 640−644.
(30) Janzen, E. G.; Wang, Y. Y.; Shetty, R. V. *J. Am. Chem. Soc.* **1978**, *100*, 2923−2925.
(31) Alberti, A.; Carloni, P.; Eberson, L.; Greci, L.; Stipa, P. *J. Chem. Soc., Perkin Trans. 2* **1997**, 887−892.
(32) Forrester, A. R.; Hepburn, S. P. *J. Chem. Soc. (C)* **1971**, *4*, 701−703.
(33) Carloni, P.; Eberson, L.; Greci, L.; Sgarabotto, P.; Stipa, P. *J. Chem. Soc., Perkin Trans. 2* **1996**, 1297−1305.
(34) Janzen, E. G.; Lin, C.-R.; Hinton, R. D. *J. Org. Chem.* **1992**, *57*, 1633−1635.
(35) Eberson, L.; McCullough, J. J.; Persson, O. *J. Chem. Soc., Perkin Trans. 2* **1997**, 133−134.
(36) Eberson, L.; McCullough, J. J. *J. Chem. Soc., Perkin Trans. 2* **1998**, 49−58.
(37) Eberson, L.; Persson, O. *J. Chem. Soc., Perkin Trans. 2* **1997**, 1689−1696.
(38) Sang, H.; Janzen, E. G.; Lewis, B. H. *J. Org. Chem.* **1996**, *61*, 2358−2363.
(39) Eberson, L. Spin trapping: Problems and artifacts. In *Toxicology of the Human Environment. The Critical Role of Free Radicals*; Rhodes, C. J., Ed.; Taylor and Francis: New York, 2000; pp 25−47.
(40) Eberson, L. *Adv. Phys. Org. Chem.* **1998**, *31*, 91−141.
(41) Bordwell, F. G.; Liu, W.-Z. *J. Am. Chem. Soc.* **2003**, *118*, 8777−8781.
(42) Iversen, P. E.; Lund, H. *Acta Chem. Scand.* **1965**, *19*, 2303−2308.
(43) Sayo, H.; Ozaki, S.; Masui, M. *Chem. Pharm. Bull. (Tokyo)* **1973**, *21*, 1988−1995.
(44) Ozaki, S.; Masui, M. *Chem. Pharm. Bull. (Tokyo)* **1978**, *26*, 1364−1369.
(45) Huie, R. E.; Neta, P. *J. Phys. Chem.* **1984**, *88*, 5665−5669.
(46) Buettner, G. R. *Arch. Biochem. Biophys.* **1993**, *300*, 535−543.
(47) Stoyanovsky, D. A.; Goldman, R.; Jonnalagadda, S. S.; Day, B. W.; Claycamp, H. G.; Kagan, V. E. *Arch. Biochem. Biophys.* **1996**, *330*, 3−11.
(48) Khramtsov, V. V.; Reznikov, V. A.; Berliner, L. J.; Litkin, A. K.; Grigor'ev, I. A.; Clanton, T. L. *Free Radic. Biol. Med.* **2001**, *30*, 1099−1107.
(49) Tuccio, B.; Lauricella, R.; Frejaville, C.; Bouteiller, J.-C.; Tordo, P. *J. Chem. Soc., Perkin Trans. 2* **1995**, 295−298.
(50) Villamena, F. A.; Zweier, J. L. *J. Chem. Soc., Perkin Trans. 2* **2002**, 1340−1344.
(51) Roubaud, V.; Sankarapandi, S.; Kuppusamy, P.; Tordo, P.; Zweier, J. L. *Anal. Biochem.* **1997**, *247*, 404−411.
(52) Khramtsov, V. V.; Weiner, L. M.; Gogolev, A. Z.; Grigor'ev, I. A.; Starichenko, V. F.; Volodarsky, L. B. *Magn. Reson. Chem.* **1986**, *24*, 199−207.
(53) Grigor'ev, I. A.; Shchukin, G. I.; Khramtsov, V. V.; Vainer, L. M.; Starichenko, V. F.; Volodarsky, L. B. *Bull. Acad. Sci. USSR, Div. Chem. Sci.* **1986**, *34*, 2169−2177.
(54) Finkelstein, E.; Rosen, G. M.; Rauckman, E. J. *Arch. Biochem. Biophys.* **1980**, *200*, 1−16.
(55) Finkelstein, E.; Rosen, G. M.; Rauckman, E. J. *Mol. Pharmacol.* **1982**, *21*, 262−265.
(56) Karoui, H.; Rockenbauer, A.; Pietri, S.; Tordo, P. *Chem. Commun.* **2002**, 3030−3031.